

# Ankle Sprains in Athletes: Current Epidemiological, Clinical and Imaging Trends

Pia M Jungmann<sup>1,2</sup>, Thomas Lange<sup>3</sup>, Markus Wenning<sup>4</sup>, Frédéric A Baumann<sup>5</sup>, Fabian Bamberg<sup>1</sup>, Matthias Jung<sup>1</sup>

<sup>1</sup>Department of Diagnostic and Interventional Radiology, Medical Center–University of Freiburg, Faculty of Medicine, University of Freiburg, Freiburg, Germany; <sup>2</sup>Department of Radiology, Kantonsspital Graubünden, Chur, Switzerland; <sup>3</sup>Department of Radiology, Medical Physics, Medical Center – University of Freiburg, Faculty of Medicine, Freiburg, Germany; <sup>4</sup>Department of Orthopedic and Trauma Surgery, Medical Center – University of Freiburg, Faculty of Medicine, Freiburg, Germany; <sup>5</sup>Department of Vascular Medicine, Hospital of Schiers, Schiers, Switzerland

Correspondence: Pia M Jungmann, Albert-Ludwigs-Universität Freiburg, Medical Center–University of Freiburg, Faculty of Medicine, University of Freiburg, Hugstetter Strasse 55, Freiburg, 79106, Germany, Tel +49 761 270-38190, Fax +49 761 270-39500, Email pia.jungmann@ksgr.ch

**Purpose:** Ankle injuries are frequent sports injuries. Despite optimizing treatment strategies during recent years, the percentage of chronification following an ankle sprain remains high. The purpose of this review article is, to highlight current epidemiological, clinical and novel advanced cross-sectional imaging trends that may help to evaluate ankle sprain injuries.

**Methods:** Systematic PubMed literature research. Identification and review of studies (i) analyzing and describing ankle sprain and (ii) focusing on advanced cross-sectional imaging techniques at the ankle.

**Results:** The ankle is one of the most frequently injured body parts in sports. During the COVID-19 pandemic, there was a change in sporting behavior and sports injuries. Ankle sprains account for about 16–40% of the sports-related injuries. Novel cross-sectional imaging techniques, including Compressed Sensing MRI, 3D MRI, ankle MRI with traction or plantarflexion-supination, quantitative MRI, CT-like MRI, CT arthrography, weight-bearing cone beam CT, dual-energy CT, photon-counting CT, and projection-based metal artifact reduction CT may be introduced for detection and evaluation of specific pathologies after ankle injury. While simple ankle sprains are generally treated conservatively, unstable syndesmotic injuries may undergo stabilization using suture-button-fixation. Minced cartilage implantation is a novel cartilage repair technique for osteochondral defects at the ankle.

**Conclusion:** Applications and advantages of different cross-sectional imaging techniques at the ankle are highlighted. In a personalized approach, optimal imaging techniques may be chosen that best detect and delineate structural ankle injuries in athletes.

**Keywords:** ankle injuries, athletic injuries, computed tomography, joint instability, magnetic resonance imaging, sprains and strains

## Introduction

The ankle joint is one of the most commonly injured joints in athletes.<sup>1,2</sup> Ankle sprains account for 40% of all sports injuries.<sup>3,4</sup> Developing common and advanced cross-sectional imaging techniques aims to detect structural lesions at the ankle and to guide therapeutic strategies. This review primarily focuses on developments, changes and adaptations in injury patterns, imaging and treatment approaches that are a current focus of orthopedic surgeons in clinical practice. Besides lateral collateral ligament injury, other potentially associated injuries including syndesmotic injuries and osteochondral lesions are discussed. For review of tendon injuries around the ankle, we refer to other publications.<sup>5–10</sup>

## Materials and Methods

For this review, an electronic search in PubMed (<http://www.ncbi.nlm.nih.gov/pubmed>) was performed to identify relevant studies that describe current trends in cross-sectional imaging after ankle sprain.

# Anatomy of Ligaments at the Ankle

The lateral collateral ligament complex at the ankle consists of three ligaments. The most anterior anterior talofibular ligament (ATFL) runs from the anterior tip of the fibula horizontally to the talar neck. In most cases, it consists of two bands.<sup>11</sup> The thin calcaneofibular ligament (CFL) runs from the lateral malleolar tip at the inferomedial border to the trochlear eminence of the calcaneus. The striated posterior talofibular ligament (PTFL) runs horizontally from the fibular malleolar fossa to the posterior talus, blending with the joint capsule. The deltoid ligament is the medial collateral ligament complex at the ankle. It consists of a deep and a superficial layer.<sup>12,13</sup> The deep layer is composed of the anterior and posterior tibiotalar ligament. The superficial layer consists of the tibiocalcaneal, the tibiospring and the tibionavicular ligament and crosses two joints. The syndesmosis consists of the anterior and posterior syndesmosis and of the interosseous ligament. The anterior syndesmosis consists of the striated anteroinferior tibiofibular ligament (AITFL) and the frequent inferior accessory fascicle (Bassett's ligament). It runs from the tibia in a slightly oblique course to the fibula.<sup>14–16</sup> The posterior syndesmosis consists of the posteroinferior tibiofibular ligament (PITFL) and its inferior part, the transverse tibiofibular ligament.<sup>17</sup> The interosseous ligament, a distal interosseous membrane expansion, runs from proximal tibial to distal fibular.<sup>18–20</sup>

## Epidemiology

Fifty-three percent of National Football League (NFL) Combine participants are reported to have a history of ankle injury.<sup>21,22</sup> Acute ankle sprain is the most common lower limb injury in athletes, accounting for 16–40% of the injuries and 14% of the emergency visits.<sup>21,23–25</sup> Ankle sprains have an incidence of 1 per 10,000 persons (8000 in Germany) per day.<sup>2,21,26</sup> In professional team sports in Germany, the ankle is the most commonly injured body part in basketball (16.9%) and handball (14.7%). Also in the FIFA World Cup 1998–2012, the ankle was the most frequently injured body part (19%).<sup>27</sup> In the 2014 Winter Olympics, the ankle was the second most commonly injured body region (12%).<sup>28</sup> During the Summer Olympics, foot and ankle injury rates ranged from 0.09 to 0.42 injuries per athlete-years (Winter Olympics: 0.02 to 0.35).<sup>23</sup> In the 2016 Summer Olympics, 8.8% of the athletes were referred for an ankle Magnetic Resonance Imaging (MRI), of which 99% had at least one abnormal finding (79% (sub)acute).<sup>29</sup>

The majority of sprains affect the lateral collateral ligament complex, which is injured in 85% of the ankle sprains.<sup>21</sup> Total ligament ruptures occur in 10% of the cases, most frequently of the ATFL (65–85%) and CFL (75–85%).<sup>21,23,30</sup> Additional injuries are osteochondral lesions, injury to the medial ligaments, the tibiofibular syndesmosis, the bifurcate ligament, the ligaments of the tarsal sinus, the peroneal tendons, and fractures.<sup>31,32</sup> The medial collateral ligament complex is more resistant to trauma than the lateral. Therefore, medial collateral ligaments injuries are far less frequent than lateral collateral ligaments and occur in 5–15% of the ankle sprains, rarely in isolation. Usually, they occur in combination with lateral ligament tears, malleolar fractures, and syndesmotic tears. In more than 50% of the cases, the superficial and the deep medial collateral ligaments are affected.

High ankle sprains include injury to the tibiofibular syndesmosis.<sup>33</sup> Injuries to the syndesmosis occur in about 10% of the ankle sprains.<sup>34</sup> Ice hockey is the most common sport to result in a high ankle sprain.<sup>35</sup> High ankle sprain results in significantly higher time to return to play (average: 41–45 days) as compared with low ankle sprain (average: 1.4 days).<sup>35</sup>

Ankle instability has a high rate of chronification.<sup>36</sup> Chronic ankle instability with persistent frequent residual symptoms, sprain recurrence and subjective ankle instability is observed in 10–40% of the cases.<sup>21,25,37,38</sup> According to van Rijn et al, 5–33% of the patients still experienced pain 1 year after ankle sprain. After 3 years, one-third of the patients reported at least one re-sprain.<sup>36</sup>

Osteochondral lesions are found in about 6–7% of the ankles after sprain,<sup>39,40</sup> in 40% of the patients with persistent ankle disability after sprain<sup>41</sup> and in 42% of the ankle MRIs in asymptomatic soccer players.<sup>42</sup> The ratio of prevalence at the talus versus tibia is about 20:1.<sup>43</sup> Two-thirds of osteochondral defects at the talus are located medially and 1/3 laterally.<sup>40,44,45</sup>

The COVID-19 pandemic has influenced sporting activity and trauma visits.<sup>46</sup> Social isolation, lack of access to facilities, spare time, home-schooling, and home-office resulted in training changes.<sup>46</sup> The running-related injury rate increased 1.4-fold.<sup>46</sup> However, only patients with severe injury showed up to the emergency room.<sup>47–49</sup> Young athletes with minor sports injuries such as ankle sprains did not seek care.<sup>47,50</sup> The percentage of patients undergoing surgery for ankle fractures remained stable.<sup>51</sup>

## Etiology

Sports injury is the cause of ankle sprain in 18% of the cases. In particular, basketball and soccer players are at risk. The injury mechanism implies plantarflexion, adduction, and inversion.<sup>15</sup>

The ATFL usually ruptures first, followed by the CFL. Due to the mechanism of the injury, PTFL ruptures as well as isolated ruptures of the CFL are extremely rare. PTFL ruptures usually only occur after ankle dislocation. Since the deltoid ligament is strong, medial malleolar fractures may occur instead of medial collateral ligament injuries. Injuries to the medial collateral ligaments usually occur in case of eversion and dorsiflexion trauma. They are usually combined with other injuries. The injury mechanism of syndesmotic injury may include external rotation of the foot, eversion of the talus and excessive dorsiflexion.<sup>33</sup> Usually, the anterior syndesmosis ruptures first. The posterior syndesmosis may stay intact. Bony avulsion of the posterior syndesmosis at the tibia corresponds to the Volkmann fracture. Injuries of the medial collateral ligament and/or to the syndesmosis require examination of the proximal fibula to exclude Maisonneuve fractures and ruptures of the interosseous membrane of the shank. Although chronic ankle instability is considered a risk factor for osteoarthritis, overall only little posttraumatic osteoarthritis is observed.<sup>37</sup> Three-dimensional (3D) stress MRI showed that the cartilage contact area in plantarflexion-supination compared to neutral-null position is reduced by about 1/3.<sup>52</sup> In patients with chronic ankle instability, the cartilage contact area is even more severely reduced (by 41% horizontal tibiotalar and 56% tibiofibular, respectively; Figure 1a and b).<sup>52</sup>

## Diagnosis

The anamnesis should imply evaluation of the trauma mechanism (supination) and recurrence. The clinical examination should imply palpation (including the fifth metatarsal and the fibular head) and range of motion. Further, the squeeze test for assessment of the syndesmosis, and the talar drawer test should be included. Be aware, that injuries to the syndesmosis are frequently overlooked at initial presentation. The clinical examination is followed by conventional radiography if one of the Ottawa Ankle rule criteria applies. Excessive imaging has been described as a common mistake in the management of ankle sprains.<sup>21</sup>

## Imaging

### Conventional Radiography

Radiography helps to rule out fractures and to evaluate the congruency of the joint including the syndesmosis. According to the Ottawa ankle rules, conventional radiography in two planes including the Mortise-view (anterior-posterior with 10° to 20° internal rotation) and the lateral view is indicated when one criterion applies:<sup>25,30,53</sup> Criteria include (i) pain at the posterior lateral malleolus (6cm), (ii) pain at the posterior medial malleolus (6cm), or (iii) impossibility of weight-bearing directly after trauma and during the examination; Criteria for conventional radiography of the foot in two planes are pain at palpation of (iv) the fifth metatarsal basis or (v) the navicular bone.<sup>30</sup> Radiography is also indicated in osteoporotic patients or medial injury. Stress radiographs are obsolete in the acute setting and are controversially discussed in case of chronic instability.<sup>38</sup>

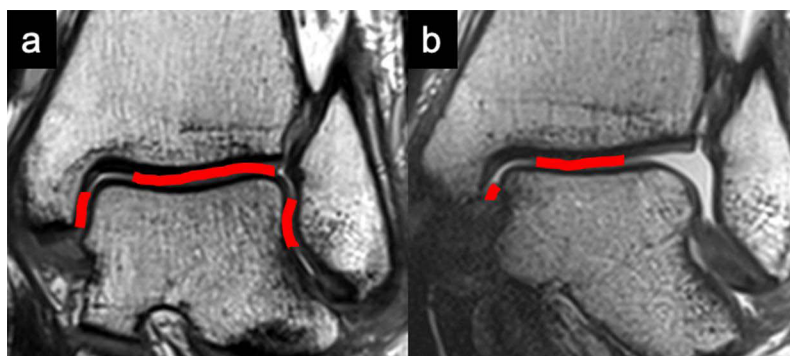


**Figure 1** Ankle Instability. (a) Coronal reconstruction of a three-dimensional MRI (intermediate weighted turbo-spin-echo) sequence in neutral position. Red indicates the cartilage contact area. (b) Coronal reconstruction of a three-dimensional MRI (intermediate weighted turbo-spin-echo) sequence in plantarflexion-supination. Red indicates the cartilage contact area. As compared to neutral position, severely reduced cartilage contact area can be observed in plantarflexion-supination.

## Computed Tomography

Computed Tomography (CT) imaging is indicated in case of suspicion for fracture but unremarkable radiography or for further evaluation of fracture lines. Performing cone-beam CT has the advantage of radiation dose reduction and evaluation under weight-bearing conditions (Figure 2a).<sup>54,55</sup> Cone-beam CT under weight-bearing is most appropriate for the evaluation of the stability of the distal tibiofibular joint under compression. The syndesmotic distance is measured at the anterior and posterior tubercles of the tibia 10mm above the joint line (Figure 2b and c). A side-to-side-difference >2mm or posterior width >6mm is considered abnormal.<sup>56,57</sup> Currently, there are no definite thresholds regarding tibiofibular displacement or malrotation.<sup>58</sup> Congruency of the distal tibiofibular joint is assumed in case of (i) harmonious elliptical line, (ii) the fibula positioned in the tibial incisura, (iii) congruent positioning of the malleoli in relation to the talus, and (iv) equal clear space.<sup>59,60</sup> Despite no definite cut-off value, malrotation can be assumed in the case of >15–20° external rotation of the fibula.<sup>61</sup> Dual-energy and photon-counting CT may have several advantages as compared to conventional CT, including assessment of BME and metal artifact reduction.<sup>62–64</sup> Dual-energy CT identifies BME around the ankle joint with a sensitivity of 88–92% and specificity of 82–93% (Figure 3a–c).<sup>65,66</sup> Besides, new iterative projection-based MAR techniques show excellent metal artifact reduction not only for soft tissue reconstructions but also for reconstructions with bone Kernel (Figure 4a and b).

## Magnetic Resonance Imaging

### Conventional MRI Sequences

Routine MRI is not recommended for simple sprains.<sup>25</sup> However, severe trauma, extreme clinical findings, suspicion of syndesmotic injury, persistent complaints, or uncertainty about the trauma mechanism may indicate cross-sectional imaging to help guide treatment.<sup>40,67</sup> Despite its low sensitivity for chronic ankle instability, also for preoperative MRI is recommended.<sup>31,38,40,41</sup> Standard high-resolution MRI protocols are suitable for patients after ankle sprain. The protocol usually

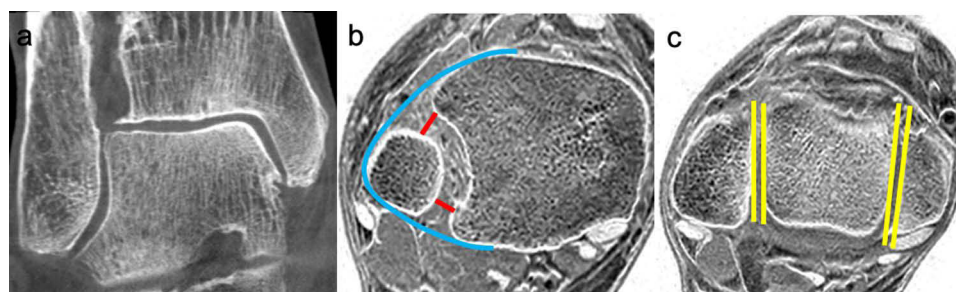


**Figure 2** Syndesmotic injury. (a) Weight-bearing cone-beam computed tomography in a patient with chronic ankle instability (coronal plane). (b) Evaluation of the syndesmotic congruency on transverse inverted TIGRE sequences 10mm proximal to the joint line in a patient with subjective persistent ankle instability. Red: anterior and posterior measurements of the width of the syndesmotic space. Blue: elliptical line. (c) Evaluation of the syndesmotic congruency on transverse inverted TIGRE sequences 6mm distal to the joint line in the same patient. Yellow: fibular rotation.

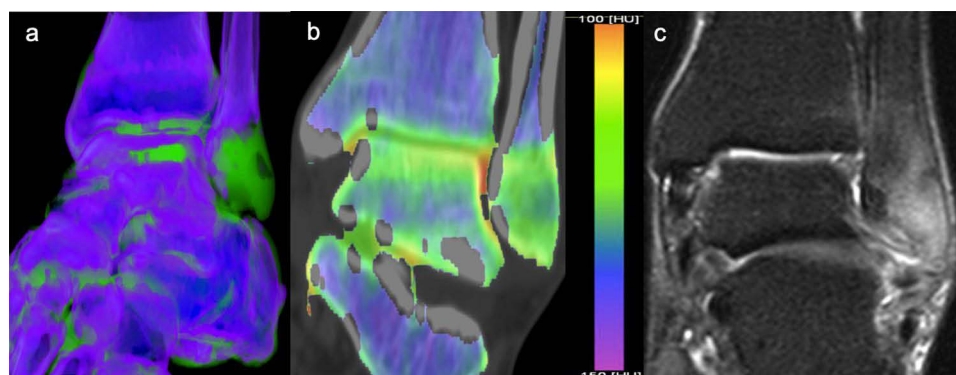


**Figure 3** Patient with bone marrow edema at the distal fibula. (a) Volume rendering of dual-energy CT with bone marrow color coding. (b) Coronal reconstructions coding of dual-energy CT with bone marrow color coding. (c) Corresponding short tau inversion recovery MRI sequence. Although visible on dual-energy CT, the bone marrow edema is still best depicted on MRI.





**Figure 4** Projection-based MAR in a patient with open reduction and internal fixation of a trimalleolar ankle fracture. Arrow: exemplary absorption artifact caused by the implant. (a) Standard CT reconstruction. (b) Projection-based MAR with Improved metal artifact reduction as compared to standard CT reconstruction. Arrow: exemplary absorption artifact caused by the implant; the artifact is reduced in projection-based MAR reconstruction images as compared to standard CT reconstruction images.

includes coronal T1-weighted (T1w) TSE images, sagittal and coronal IMw fat-saturated (fs) TSE images, and transverse images either IMw fs or T2w (or both) TSE images, all with a slice thickness of  $\leq 3\text{mm}$ . It is important to keep the echo time (TE) between 35 and 50ms for IMw sequences to mitigate “magic angle” artifacts.<sup>68</sup> Acquiring images at two echo times may be useful in case of collateral ligament injuries. Fat suppression by the use of short-tau-inversion-recovery (STIR) sequences may be of advantage in cases with metal implants. Dixon sequences allow reconstruction of images with and without fat suppression.<sup>68</sup> Since the tibiofibular syndesmosis has an oblique course, some radiologists recommend additional oblique transverse images, especially in cases with clinical suspicion of a syndesmotic injury.<sup>69</sup> Alternatively, these oblique transverse images may be reconstructed from a 3D TSE sequence with no difference in accuracy (Figure 5).<sup>70–72</sup> 3D GRE sequences are inferior in depicting BME and therefore not suitable for the standard ankle protocol.<sup>73,74</sup> Superiority of 3T and 7T over 1.5T MRI of the ankle with higher resolution was described.<sup>73</sup> However, 7T only surpassed 1.5T ankle MRI for GRE sequences in runners. Tibiotalar bone edema-like lesions were

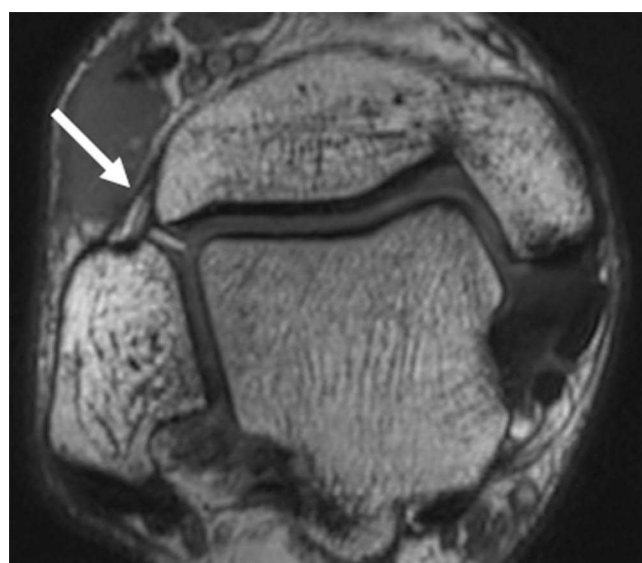


**Figure 5** Oblique reconstructions for improved evaluation of the anterior syndesmosis from three-dimensional intermediate weighted turbo-spin-echo images. Arrow: anteroposterior tibiofibular ligament (anterior syndesmosis).

barely visible at 7T.<sup>73</sup> Using compressed sensing (CS) with slice-encoding for metal artifact correction (SEMAC) may result in excellent in-plane and through-plane artifact reduction,<sup>75–78</sup> superior to high-bandwidth techniques for the evaluation of bone, BME, tendons, and the joint capsule in patients with total ankle arthroplasty or other large metallic implants (Figure 6a–d).<sup>76</sup> In the case of small implants, standard TSE sequences or high bandwidth sequences should be used, since the image quality of CSSEMAC sequences is still inferior.<sup>78</sup> At the ankle, the CS techniques may be combined with TSE, Dixon, and T2-mapping sequences without loss of image quality.<sup>79,80</sup>

### Collateral Ligaments

Of the lateral collateral ligaments, the ATFL and the CFL have a hypointense signal on MR imaging and a linear shape.<sup>81</sup> The strong PFTL has a striated, fan-like shape caused by fibrofatty components. Of the medial collateral ligaments, the thick, striated posterior tibiotalar ligament, the tibiocalcaneal ligament, the tibiospring ligament and the tibionavicular ligament can usually be identified on MRI. The anterior tibiotalar ligament cannot always be identified.<sup>12,13</sup> Periligamentous edema and increased signal intensity, loss of striation as well as partial discontinuity indicate partial ruptures.<sup>12</sup> Ligament discontinuity indicates complete ruptures. The overall accuracy of MRI for partial and complete tears of the ATFL is 74% and 79%, respectively (CFL: 66% and 88%, respectively).<sup>82</sup> Tears usually occur in the middle third of the ligaments or at the talar or calcaneal insertion, respectively.<sup>81</sup> After 3 months, evaluation on MRI is difficult with a decreasing accuracy due to scarring. For chronic ankle instability, increased ATFL length and width, as well as large angles between ATFL and PFTL, have been described.<sup>83,84</sup> Still, the sensitivity for the detection of collateral ligament lesions is low in chronic cases (28–38%).<sup>31</sup> Higher SNR of injured ATFL compared to controls and correlations of higher SNR with remnant condition, reparability, and outcomes are reported.<sup>83,85,86</sup> However, using SNR for

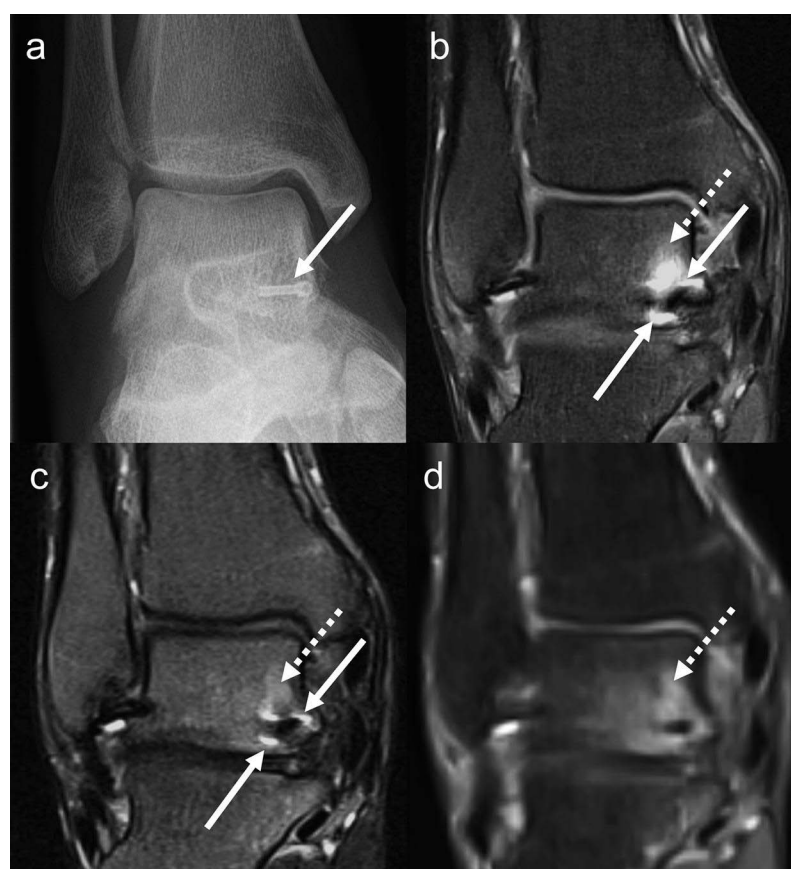


**Figure 6** Metal artifact reduced 1.5T MRI of the ankle. Patient with previous screw fixation for fracture. (a) Anteroposterior radiography; arrow: screw. (b) Coronal intermediate weighted turbo spin-echo sequence with fat saturation. Hyperintense susceptibility artifacts adjacent to the screw (arrows) obscure BME (dotted arrow). (c) MARS STIR sequence view-angle-tilting. Differentiation between BME (dotted arrow) and artifact (arrows) is challenging. (d) CSSEMAC STIR sequence susceptibility artifacts are entirely eliminated. True BME is revealed (dotted arrow). Image resolution and quality however are reduced. Therefore, application of SEMAC should only be considered if the structures to be evaluated are in close proximity to large metal implants.

**Abbreviations:** BME, bone marrow edema; MARS, metal artifact reducing sequences; STIR, short tau inversion recovery; CSSEMAC, compressed sensing slice encoding for metal artifact correction.

quantitative measurements remains questionable. For more sophisticated quantitative measurements of ligament signal intensity at the ankle, UTE-based T2\* values are being used.<sup>87</sup>

## Syndesmosis

The anterior and posterior syndesmosis usually have a fascicular appearance on MRI. Thickening, increased signal, loss of fascicular appearance, and soft tissue swelling indicate partial rupture of the syndesmosis. Discontinuity, retraction, or curved appearance indicate complete rupture of the syndesmosis. In the acute setting, tibiotalar joint effusion indicates syndesmotic injury.<sup>88</sup> Differentiating between disruption and syndesmotic instability is challenging.<sup>58</sup> Bone contusions are seen in >2/3 of syndesmotic injuries.<sup>34</sup> Posterior malleolus BME (in 60%) and posterior malleolus fracture (in 16%) indicate posterior syndesmosis rupture and consecutive instability.<sup>72</sup> The sensitivity of MRI decreases from 94% for <6 weeks to 54% for >12 weeks after injury.<sup>72</sup>

## Osteochondral Lesions

Generally, posteromedial osteochondral lesions are associated with chronic instability, while lateral lesions are more likely to be the result from acute trauma. Medial defects are usually located posteromedially with a deep osseous involvement based on osteochondral compression.<sup>44,68</sup> Lateral talar defects are usually located anterolaterally or midlaterally with superficial cartilage delamination or flake fracture based on shearing injury.<sup>44</sup> At the tibia, there is no preferred location.<sup>89</sup> Regularly at the anteromedial tibial plafond, an osteochondral concavity can be observed (Notch of Harty; Figure 7a).<sup>90</sup> Biochemical quantitative MR techniques may help to detect cartilage degeneration and cartilage defects (Figure 7a and b). Higher relaxation times indicate more severe cartilage matrix degeneration (see below). The sensitivity for the detection of cartilage lesions at the talus is about 50–75% for conventional MRI,<sup>74</sup> 75–87% for MR arthrography (MRA)<sup>91</sup> and 89–92% for CT arthrography (CTA; Figure 7c and d).<sup>74,91</sup> If lesions are detected on MRI, defect size is overestimated (52%) or underestimated (24%) in many cases.<sup>92</sup> A non-invasive method for optimized cartilage evaluation is MRI under axial traction (Figure 7e and f). The radiographic Berndt and Harty classification for osteochondral lesions was transferred to MRI by Nelson and Dipaola (Figure 8).<sup>93–95</sup> The grades are associated with pain intensity.<sup>96</sup> It is clinically important to differentiate between stable grade II (demarcation of the fragment/

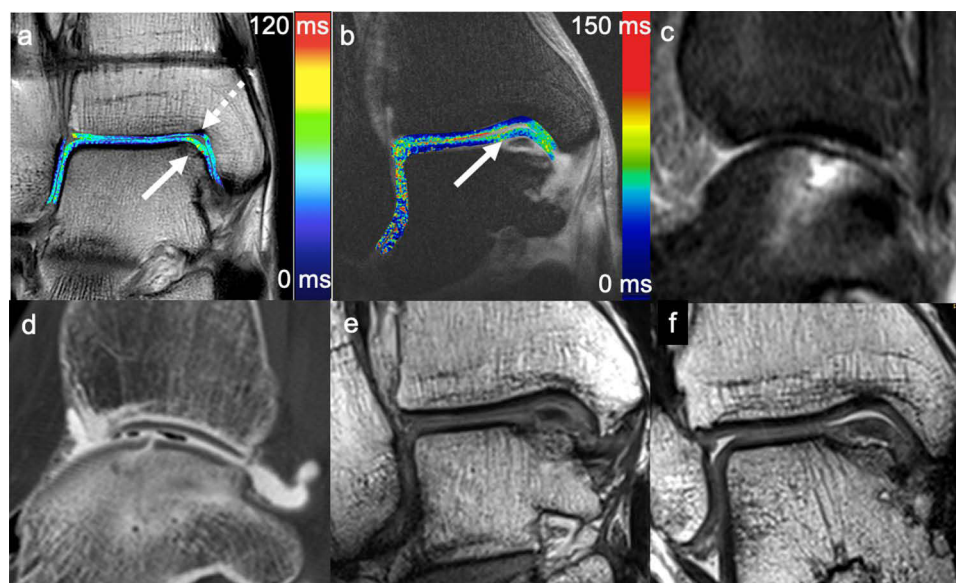


**Figure 7** Cross-sectional imaging of osteochondral defects. (a) Coronal T2 multi-slice multi-echo spin-echo sequence in a patient after suture-button fixation for syndesmotic instability. Color-coded cartilage T2 map overlaid on first echo image. Osteochondral defect with higher T2 values at the medial talar dome (arrow). The Notch of Harty at the anteromedial tibia (dotted arrow). (b) Patient with an osteochondral lesion at the medial talar dome. Coronal multi-slice multi-echo T1 rho cartilage color maps overlaid on first echo image demonstrate increased cartilage relaxation times in the osteochondral lesion (arrow). (c) Sagittal STIR MRI sequence of a patient with an osteochondral lesion at the talus (same patient as d). Subchondral BME is nicely depicted while the presence of a chondral defect can only be suggested. (d) CT arthrography of the same patient as c. The fissural osteochondral defect that causes the BME can be appreciated. (e) Coronal reconstructions of 3D IMw TSE images of a patient with an osteochondral lesion at the medial talar dome (same patient as b and f). Without traction a grade 2 lesion without fragment loosening is assumed. (f) Coronal reconstructions of 3D IMw TSE images of the same patient as in b and e with axial traction of the ankle. Images with axial traction reveal subchondral delamination with fluid interposition leading to classification grade 3 and representing an indication for surgical cartilage repair. **Abbreviations:** BME, bone marrow edema; STIR, short tau inversion recovery (same patient as b and e).

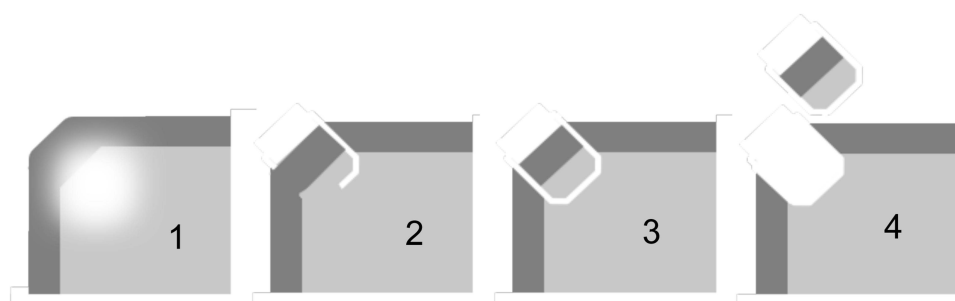


**Figure 8** Grading of osteochondral lesions at the ankle according to Nelson and Dipaola. Grade 1: Cartilage swelling. Subchondral signal changes. Grade 2: Subchondral fragment demarcation. Cartilage possibly fractured. Grade 3: Cartilage fractured; fluid between fragment and local bone (unstable). Grade 4: Free intraarticular body.

partial loosening) and unstable grade III (total loosening, surgical treatment indicated).<sup>97</sup> Indirect signs for osteochondral involvement at the talus include joint effusion,<sup>88</sup> cartilage signal changes, and subchondral BME. Frequently, subchondral BME is the only indicator of talar cartilage defect on MRI.<sup>74,98</sup>

### Bone Marrow Edema

As a common finding after an ankle injury, BME helps determine the trauma mechanism.<sup>98</sup> Following inversion injury, BME involves the lateral malleolus, the medial talus, and the medial tibia.<sup>98</sup> After ankle sprain, BME and osteophytes were associated with swelling, reduced plantarflexion, and pain.<sup>99</sup> BME of the medioplantar talar head is associated with severe ligamentous injury in ankle sprain, in particular to the medial and lateral collateral ligament complex.<sup>100</sup> Avulsion injuries are difficult to detect on MRI since they are not always accompanied by a BME.

### Chronic Ankle Instability

Interestingly, MR imaging findings do not correlate with return to play following an ankle sprain.<sup>35</sup> Imaging findings in patients with persistent ankle instability are mainly ATFL injuries (54%) and osteochondral changes (40%) including cartilage lesions, osteophytes, and BME.<sup>41,99</sup> To assess osteoarthritis on MRI, semi-quantitative scoring methods have been developed for the knee (WORMS),<sup>101</sup> the shoulder (SOAS),<sup>102</sup> the hip (SHOMRI),<sup>103</sup> and also for the ankle (Ankle Osteoarthritis Scoring System, AOSS).<sup>104</sup>

### Pre-Signing MRI

Imaging, including MRI of the ankle, plays an increasing role in pre-signing medical examination.<sup>105</sup> Working closely with the clinicians and being aware of the high prevalence of findings and ethical and medicolegal issues is required.<sup>105</sup> In professional soccer players, a high prevalence of asymptomatic osteochondral lesions in at least one of the joints of the foot and ankle was described (Figure 9a and b). Seventeen percent of all players showed cartilage lesions with >50% lesion depth. Subchondral bone marrow edema was present in all of these cases.<sup>42</sup> Eighty-seven percent of players

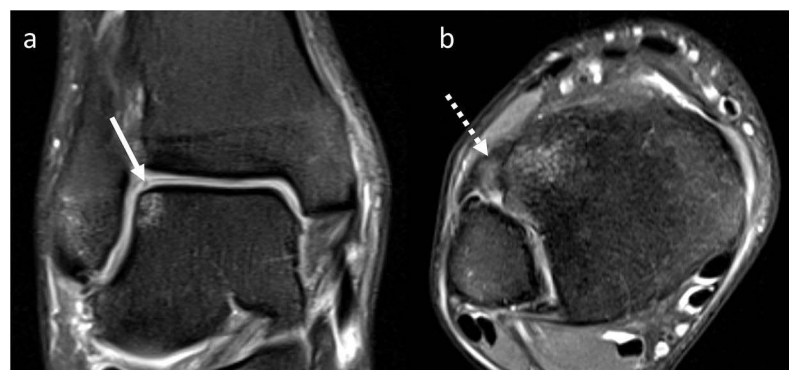


**Figure 9** Pre-signing MRI. MRI of an elite athlete using coronal (a) and transverse (b) intermediate weighted turbo spin-echo sequences. Prevalent partial thickness cartilage defect with adjacent subchondral bone marrow edema at the lateral talar dome (arrow). Elongation, thickening and signal increase of the anterior tibiofibular ligament after previous rupture (dotted arrow).



showed degenerative joint disease (Mostly Kellgren–Lawrence grade 1) and 64% synovitis. Tibiotalar cartilage T2\* values are increased in football players.<sup>106</sup> Half of the NFL Combine participants were shown to have signs of osteoarthritis around the ankle joint.<sup>21,22</sup>

### Biochemical Cartilage MRI

Quantitative MRI techniques were applied for cartilage imaging at the ankle to assess cartilage matrix quality, cartilage stress, and early degeneration. Running, lateral ankle instability, and osteochondral lesions result in increased tibiotalar or subtalar cartilage T2, T2\* or T1rho relaxation times.<sup>107–113</sup> Combined ATFL and CFL rupture resulted in higher T2 values with worse clinical scores than isolated injury.<sup>108,111</sup> Early cartilage matrix degeneration was not halted by ATFL repair or reconstruction.<sup>114</sup>

### CT-Like MRI

Several new MR imaging techniques with CT-like image impression have been published, such as zero echo time (ZTE), ultra-short echo time (UTE), or 3D T1w spoiled gradient-echo MRI (T1GRE) sequences, which may all be applied at the ankle (Figure 10a–c).<sup>115–118</sup> However, all techniques currently still have their limitations. Inverted T1GRE sequences are easiest to acquire and have the highest spatial resolution and image contrast.<sup>116,119</sup> As a disadvantage, not only bone is depicted bright on inverted images but also fluid, ligaments, and tendons. Therefore, detection of tendon calcifications or avulsion fractures is still challenging on T1GRE sequences. BME cannot be differentiated from sclerosis.<sup>119</sup> On UTE images, tendons may be differentiated from bone, sclerosis, and calcification, but ligaments and fluid still appear bright.<sup>116,118–121</sup> Disadvantages are motion artifacts, blurring, signal inhomogeneity, low SNR, lower diagnostic image quality, and long acquisition times.<sup>119,122</sup> ZTE is most promising for bone imaging on MRI since only calcified structures are shown bright.<sup>123–125</sup> BME, ligaments, and tendons can be differentiated from bone, sclerosis, and calcifications. It also has reduced acoustic noise levels. Still, ZTE images have severe chemical shift artifacts, low SNR, and image quality, although cortical delineation, cortical thickness, and pathology visualization were reported similar to CT<sup>126</sup> with good performance for the shoulder,<sup>124,127</sup> and hip.<sup>123</sup> For the ankle joint, 3D intermediate-weighted (IMw) turbo spin-echo (TSE) sequences and T1GRE sequences were applied so far.<sup>57,117</sup>

### Ultrasonography

In doubt of syndesmotic injury, complementary stress ultrasonography is recommended.<sup>128</sup> After acute ankle sprain, ultrasonography may be used for evaluation of superficial tendons, ligaments and muscles, while it is inadequate for the evaluation of deeper structures,<sup>129</sup> for evaluation of the lateral collateral ligaments and the anterior syndesmosis standardized ultrasound may replace MRI.<sup>130</sup> A high correlation of ligament injuries detected was reported for the two modalities. However, ultrasonography is investigator dependent and should be performed by an experienced sonographer.

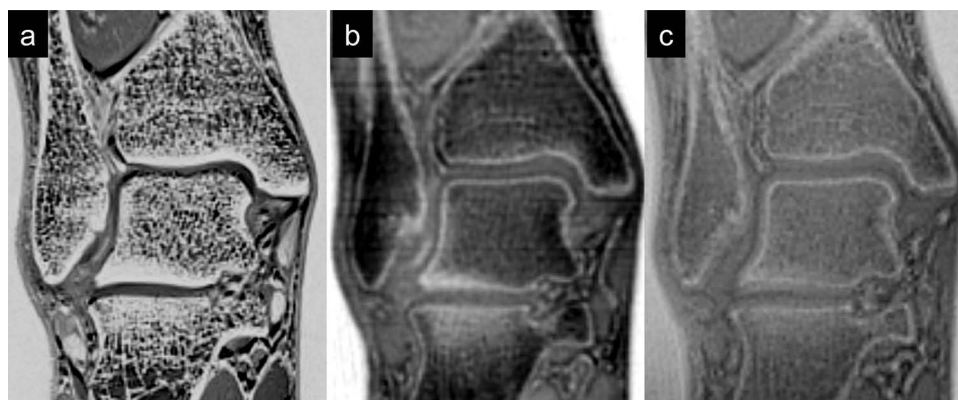


**Figure 10** CT-like MRI of the ankle. Coronal reconstructions. (a) 3D T1w spoiled gradient-echo MR; (b) ultra-short echo time imaging; (c) zero echo time imaging.

## Treatment

In recent decades, the most common therapy of ankle sprains shifted from surgical to conservative treatment including early functional training, with bracing and physiotherapy.<sup>21,25,30</sup> After initial treatment according to the “RICE” regime with rest, ice, compression and elevation, the treatment strategy depends on the severity of the injury. Grade I is defined by sprain and partial rupture of the lateral collateral ligaments and is functionally treated with tape for 4 to 6 weeks with weight bearing as tolerated. Grade II is defined by total rupture of the LFTA and LFC and is treated with orthosis for 6 weeks and weight bearing as tolerated. Grade III is defined by rupture of the collateral ligaments plus additional medial collateral ligament injury or/and additional other concomitant injuries. In case of grade III injuries, immobilization for a maximum of 10 days may be of advantage, followed by functional treatment in an orthosis until 6 weeks after injury.<sup>30</sup> Despite the high rate of chronification, the majority of cases remain on conservative therapy after 6 months.<sup>21,25,37,38</sup> External stabilization of the ankle during sports is recommended for at least 1 year following an index sprain, and even longer in chronic instability if functional training and compensation for mechanical deficits is insufficient (so-called Non-Copers).<sup>131</sup> Physiotherapy is helpful in case of recurrence and persistent instability including strengthening and proprioception training. A recent review and meta-analysis evaluated the effects of Kinesio Taping on sports performances and ankle functions in athletes with chronic ankle instability.<sup>132</sup> The authors report a stabilizing effect of ankles with significant improvement in gait functions, reduction in inversion and eversion range of motion, decrease in the muscle activation of the long peroneus and decrease in the postural sway in movement in the mid-lateral direction.<sup>132</sup>

## Surgery

Isolated total ruptures of lateral collateral ligaments may only be treated surgically in high-level athletes with severe instability.<sup>38</sup> Nowadays, also isolated ruptures of the anterior syndesmosis are treated conservatively if the distal tibiofibular congruency (eg, on weight-bearing cone-beam CT) is maintained. Additional ruptures of the interosseous membrane or the posterior syndesmosis with consecutive instability and/or chronic pain may require surgery.<sup>57,133</sup> Other indications for surgery include interposition of lateral collateral ligaments, (osteo)chondral lesions, impingement, and obviously dislocated fractures.<sup>38</sup>

When surgery is indicated, lateral collateral ligament repair is the treatment of choice.<sup>38</sup> In chronic cases, surgical reconstruction may be considered (modified Brostrom procedure).<sup>25,134–136</sup> It implies refixation of the scar tissue to the lateral malleolus with or without up to three intraosseous suture anchors.<sup>137,138</sup> In case of treatment failure, generalized laxity, or poor ligament quality, lateral ligament reconstruction (using gracilis autograft or allograft) of both the ATFL and CFL should be considered.<sup>38,134</sup> Reconstruction has the risk of overconstraint which may produce a feeling of tightness of the ankle, which is not observed after repair, and may result in early osteoarthritis.<sup>139</sup> Alternative or additional therapeutic approaches include platelet-rich plasma (PRP) injections, which can stimulate tissue healing.<sup>37</sup>

For surgical treatment of syndesmotic injury, advantages of suture-button fixation systems over screw fixation are (i) no screw removal, (ii) early functional rehabilitation with immediate full weight bearing, and (iii) better outcomes with earlier return-to-sport.<sup>67</sup> Despite the decreased incidence of malreduction, elongation of the tight rope can occur. Therefore, initial overcorrection is required. Intermittent trends towards double-suture-button fixation were abandoned due to insufficient superiority.

Although nonoperative treatment can be considered a good option for patients with OCL at the talus.<sup>140</sup> OCL lesion size at the talus increased by 11% within 3 to 10 years.<sup>140</sup> In symptomatic patients, cartilage repair surgery is considered treatment of choice.<sup>45,141–143</sup> None of the surgical strategies is superior.<sup>141,144–148</sup> “Magnetic Resonance Observation of Cartilage Repair Tissue” (MOCART) scores vary around 60 with frequent BME, cysts, underfilling, and tissue irregularities.<sup>147,149–157</sup> BME may have an impact on clinical outcomes.<sup>155,156</sup> Although after matrix-associated chondrocyte implantation (MACI) better filling has been reported,<sup>157</sup> need for early return-to-sports leads to extensive use of microfracturing or Autologous Matrix-Induced Chondrogenesis (AMIC; microfracturing plus collagen I/III matrix). Autologous osteochondral transplantation (OCT) is a good option for large defects.<sup>149,158</sup> The newest technique is minced cartilage implantation.<sup>146</sup> Briefly, intact native hyaline cartilage is minced into small pieces with a specific device or knife, mixed with PRP, filled as a paste-like mixture into the defect, and covered with thrombinator/fibrin glue (Figure 11a–d).<sup>146</sup>

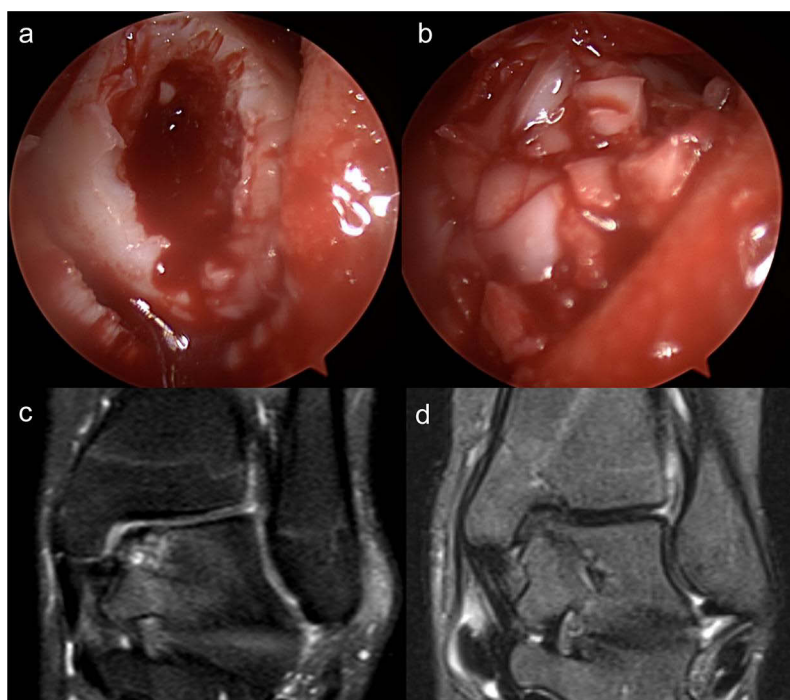


**Figure 11** Minced cartilage implantation. Minced cartilage implantation at the ankle in a patient with osteochondral defect and failed retrograde drilling. (a) Arthroscopic image of the osteochondral defect before surgery. (b) After minced cartilage implantation the defect is filled with healthy cartilage fragments embedded in PRP-mixture and covered with fibrin glue. (c) Preoperative coronal intermediate weighted fat-saturated MRI demonstrating the osteochondral defect at the medial talar dome. (d) Postoperative short tau inversion recovery MRI with completely resolved subchondral bone marrow edema and cartilage repair tissue.

## Discussion

There is a high prevalence of ankle injuries during the Olympic Games and other big tournaments. Ankle sprain is the most common injury. After clinical examination, conventional radiography should be performed according to the Ottawa ankle rules. A summary of new technical developments of cross-sectional imaging that may help in the context of imaging after ankle sprain is provided in Table 1. Cone-beam CT is the imaging method of choice to evaluate the

**Table 1** New Technical Developments of Cross-Sectional Imaging May Help in the Context of Imaging After Ankle Sprain

Technique	Applications/Advantages	Disadvantages
Cone-beam CT	Reduced radiation dose; under weight-bearing	Increased artifacts, particularly in case of metal implants
Dual-energy-CT	BME detection; MARS	Increased radiation dose
Photon-counting CT	Low radiation dose; BME detection; MARS	Availability
Projection-based MAR CT	MARS	Specific artifacts
CT-like MRI	No need for CT	All techniques have limitations
CSSEMAC MRI	MARS	Poor resolution and contrast, reconstruction-time
3D IMw TSE	Reconstruction in every direction	Fast scan times and good quality only without fat saturation
CT arthrography	High accuracy for osteochondral defects	Invasive
Traction MRI	Cartilage surface depiction improved; non-invasive	Time-consuming; not feasible: overweight, osteoarthritis
Plantarflexion-supination MRI	Objectification of instability	Time-consuming; availability
Quantitative relaxation time	High sensitivity for cartilage matrix degeneration	Limited to early degeneration

**Abbreviations:** CT, computed tomography; MRI, magnetic resonance imaging; 3D IMw TSE, three-dimensional intermediate weighted turbo-spin echo; BME, bone marrow edema; MAR, metal artifact reduction; MARS, metal artifact reduction sequences.

congruency and instability of the distal tibiofibular joint under weight-bearing conditions. BME may be detected by the use of dual-energy or photon-counting CT. In case of severe injury, early MRI is recommended since the sensitivity for the detection of structural defects decreases over time. Advanced MR techniques using native and stress 3D IMw TSE sequences of the ankle may help in the evaluation of chronic ankle instability. While CTA is currently the method of choice for the evaluation of osteochondral lesions at the ankle, MRI with axial traction may represent a good non-invasive alternative. Early cartilage matrix degeneration in patients with chronic ankle instability and osteochondral lesions may be detected via quantitative MR imaging techniques. More advanced degenerative changes may be assessed using the AOSS. Complementing MRI with CT-like images may help detect osseous abnormalities. Stress ultrasonography helps in doubt of syndesmotic injury. Ultrasonography may detect injuries to the lateral collateral ligaments and the syndesmosis reliably when performed by experienced investigators. In case of ankle sprain in athletes, besides looking for ruptures of the lateral collateral ligaments, it is most important to pay attention to additional injuries of the bone, the syndesmosis, the medial collateral ligaments, osteochondral injuries, and tendons to guide clinical treatment decisions. There was a paradigm shift towards conservative treatment for ankle sprain and syndesmotic injuries with an emphasis on secondary prevention. The current surgical treatment of unstable syndesmoses is single suture-button fixation. Besides microfracturing and AMIC, minced cartilage implantation represents a new cartilage repair technique.

## Conclusion

Advanced cross-sectional imaging techniques at the ankle that best detect and delineate structural and ultrastructural abnormalities may be applied in a dedicated, personalized approach after ankle injury in athletes.

## Abbreviations

AITFL, anteroinferior tibiofibular ligament; AMIC, autologous matrix-induced chondrogenesis; AOSS, Ankle Osteoarthritis Scoring System; ATFL, anterior talofibular ligament; BME, bone marrow edema; CFL, calcaneofibular ligament; COVID-19, coronavirus disease 2019; CS, compressed sensing; CT, computed tomography; CTA, CT arthrography; FIFA, Fédération Internationale de Football Association; MACI, matrix-associated chondrocyte implantation; MAR, metal artifact reduction; MARS, metal artifact reduction sequences; MOCART, magnetic resonance observation of cartilage repair tissue; MRA, MR arthrography; MRI, magnetic resonance imaging; NFL, National Football League; OCT, autologous osteochondral transplantation; PD, proton density weighted; PITFL, posteroinferior tibiofibular ligament; PRP, platelet-rich plasma; PTFL, posterior talofibular ligament; SEMAC, slice-encoding for metal artifact correction; SNR, signal-to-noise ratio; SOAS, shoulder osteoarthritis severity; TSE, turbo spin echo; T1GRE, T1w spoiled gradient-echo; UTE, ultra-short echo time, WOMS, Whole-Organ Magnetic Resonance Imaging Score; ZTE, zero echo time; 3D, three-dimensional; 3T, three Tesla; 7T, seven Tesla.

## Acknowledgments

We acknowledge support by the Open Access Publication Fund of the University of Freiburg. The author MJ is supported by the Berta-Ottenstein-Program for Clinician Scientists, Faculty of Medicine, University of Freiburg.

## Author Contributions

All authors made a significant contribution to the work reported (conception, study design, execution, acquisition of data, analysis and/or interpretation). All authors have drafted, written, and/or substantially revised and/or critically reviewed the article. All authors have agreed on the journal to which the article will be submitted. All authors reviewed and agreed on all versions of the article before submission, during revision, the final version accepted for publication, and any significant changes introduced at the proofing stage. All authors agree to take responsibility and be accountable for the contents of the article.

## Funding

This work was funded by the German Society of Musculoskeletal Radiology (Deutsche Gesellschaft für muskuloskelettale Radiologie; DGMSR).



## Disclosure

Prof. Dr. Fabian Bamberg reports grants, personal fees from Bayer Healthcare and Siemens Healthineers, during the conduct of the study. The authors report no other conflicts of interest in this work.

## References

1. Patel P, Russell TG. *Ankle Radiographic Evaluation*. Treasure Island (FL): StatPearls; 2021.
2. Holmer P, Sondergaard L, Konradsen L, Nielsen PT, Jorgensen LN. Epidemiology of sprains in the lateral ankle and foot. *Foot Ankle Int*. 1994;15(2):72–74. doi:10.1177/107110079401500204
3. Huch K, Kuettner KE, Dieppe P. Osteoarthritis in ankle and knee joints. *Semin Arthritis Rheum*. 1997;26(4):667–674. doi:10.1016/S0049-0172(97)80002-9
4. Johnson VL, Giuffre BM, Hunter DJ. Osteoarthritis: what does imaging tell us about its etiology? *Semin Musculoskelet Radiol*. 2012;16(5):410–418. doi:10.1055/s-0032-1329894
5. Maffulli N, Longo UG, Kadakia A, Spiezia F. Achilles tendinopathy. *Foot Ankle Surg*. 2020;26(3):240–249. doi:10.1016/j.fas.2019.03.009
6. Dams OC, van den Akker-Scheek I, Diercks RL, Wendt KW, Zwerver J, Reininga IHF. Surveying the management of Achilles tendon ruptures in the Netherlands: lack of consensus and need for treatment guidelines. *Knee Surg Sports Traumatol Arthrosc*. 2019;27(9):2754–2764. doi:10.1007/s00167-018-5049-5
7. Jackson LT, Dunaway LJ, Lundeen GA. Acute tears of the tibialis posterior tendon following ankle sprain. *Foot Ankle Int*. 2017;38(7):752–759. doi:10.1177/1071100717701686
8. Dams OC, Reininga IHF, Gielen JL, van den Akker-Scheek I, Zwerver J. Imaging modalities in the diagnosis and monitoring of Achilles tendon ruptures: a systematic review. *Injury*. 2017;48(11):2383–2399. doi:10.1016/j.injury.2017.09.013
9. Schweitzer ME, Karasick D. MR imaging of disorders of the Achilles tendon. *AJR Am J Roentgenol*. 2000;175(3):613–625. doi:10.2214/ajr.175.3.1750613
10. Mengiardi B, Pinto C, Zanetti M. Spring ligament complex and posterior tibial tendon: MR anatomy and findings in acquired adult flatfoot deformity. *Semin Musculoskelet Radiol*. 2016;20(1):104–115. doi:10.1055/s-0036-1580616
11. Choo HJ, Lee SJ, Kim DW, Jeong HW, Gwak H. Multibanded anterior talofibular ligaments in normal ankles and sprained ankles using 3D isotropic proton density-weighted fast spin-echo MRI sequence. *AJR Am J Roentgenol*. 2014;202(1):W87–94. doi:10.2214/AJR.13.10727
12. Mengiardi B, Pinto C, Zanetti M. Medial collateral ligament complex of the ankle: MR imaging anatomy and findings in medial instability. *Semin Musculoskelet Radiol*. 2016;20(1):91–103. doi:10.1055/s-0036-1580617
13. Lee S, Lin J, Hamid KS, Bohl DD. Deltoid ligament rupture in ankle fracture: diagnosis and management. *J Am Acad Orthop Surg*. 2019;27(14):e648–e658. doi:10.5435/JAAOS-D-18-00198
14. Subhas N, Vinson EN, Cothran RL, Santangelo JR, Nunley JA, Helms CA. MRI appearance of surgically proven abnormal accessory anterior-inferior tibiofibular ligament (Basset's ligament). *Skeletal Radiol*. 2008;37(1):27–33. doi:10.1007/s00256-007-0390-7
15. Sharif B, Welck M, Saifuddin A. MRI of the distal tibiofibular joint. *Skeletal Radiol*. 2020;49(1):1–17. doi:10.1007/s00256-019-03260-7
16. Oae K, Takao M, Naito K, et al. Injury of the tibiofibular syndesmosis: value of MR imaging for diagnosis. *Radiology*. 2003;227(1):155–161. doi:10.1148/radiol.2271011865
17. Golano P, Vega J, de Leeuw PA, et al. Anatomy of the ankle ligaments: a pictorial essay. *Knee Surg Sports Traumatol Arthrosc*. 2010;18(5):557–569. doi:10.1007/s00167-010-1100-x
18. Williams BT, Ahrberg AB, Goldsmith MT, et al. Ankle syndesmosis: a qualitative and quantitative anatomic analysis. *Am J Sports Med*. 2015;43(1):88–97. doi:10.1177/0363546514554911
19. Boonthathip M, Chen L, Trudell DJ, Resnick DL. Tibiofibular syndesmosis ligaments: MR arthrography in cadavers with anatomic correlation. *Radiology*. 2010;254(3):827–836. doi:10.1148/radiol.09090624
20. Lilyquist M, Shaw A, Latz K, Bogener J, Wentz B. Cadaveric analysis of the distal tibiofibular syndesmosis. *Foot Ankle Int*. 2016;37(8):882–890. doi:10.1177/1071100716643083
21. Halabchi F, Hassabi M. Acute ankle sprain in athletes: clinical aspects and algorithmic approach. *World J Orthop*. 2020;11(12):534–558. doi:10.5312/wjo.v11.i12.534
22. Mulcahey MK, Bernhardtson AS, Murphy CP, et al. The epidemiology of ankle injuries identified at the National Football League Combine, 2009–2015. *Orthop J Sports Med*. 2018;6(7):2325967118786227. doi:10.1177/2325967118786227
23. Sharma S, Dhillon MS, Kumar P, Rajnish RK. Patterns and trends of foot and ankle injuries in Olympic athletes: a systematic review and meta-analysis. *Indian J Orthop*. 2020;54(3):294–307. doi:10.1007/s43465-020-00058-x
24. Fong DT, Man CY, Yung PS, Cheung SY, Chan KM. Sport-related ankle injuries attending an accident and emergency department. *Injury*. 2008;39(10):1222–1227. doi:10.1016/j.injury.2008.02.032
25. Scillia AJ, Pierce TP, Issa K, et al. Low ankle sprains: a current review of diagnosis and treatment. *Surg Technol Int*. 2017;30:411–414.
26. Waterman BR, Owens BD, Davey S, Zacchilli MA, Belmont PJ. The epidemiology of ankle sprains in the United States. *J Bone Joint Surg Am*. 2010;92(13):2279–2284. doi:10.2106/JBJS.I.01537
27. Junge A, Dvorak J. Injury surveillance in the World Football Tournaments 1998–2012. *Br J Sports Med*. 2013;47(12):782–788. doi:10.1136/bjsports-2013-092205
28. Nabhan D, Walden T, Street J, Linden H, Moreau B. Sports injury and illness epidemiology during the 2014 Youth Olympic Games: United States Olympic Team Surveillance. *Br J Sports Med*. 2016;50(11):688–693. doi:10.1136/bjsports-2015-095835
29. Heiss R, Guermazi A, Jarraya M, et al. Prevalence of MRI-detected ankle injuries in athletes in the Rio de Janeiro 2016 summer Olympics. *Acad Radiol*. 2019;26(12):1605–1617. doi:10.1016/j.acra.2019.02.001
30. Vuurberg G, Hoorntje A, Wink LM, et al. Diagnosis, treatment and prevention of ankle sprains: update of an evidence-based clinical guideline. *Br J Sports Med*. 2018;52(15):956. doi:10.1136/bjsports-2017-098106
31. Staats K, Sabeti-Aschraf M, Apprich S, et al. Preoperative MRI is helpful but not sufficient to detect associated lesions in patients with chronic ankle instability. *Knee Surg Sports Traumatol Arthrosc*. 2018;26(7):2103–2109. doi:10.1007/s00167-017-4567-x

32. Hintermann B, Boss A, Schafer D. Arthroscopic findings in patients with chronic ankle instability. *Am J Sports Med.* 2002;30(3):402–409. doi:10.1177/03635465020300031601
33. Delahunt E, Bleakley CM, Bossard DS, et al. Clinical assessment of acute lateral ankle sprain injuries (ROAST): 2019 consensus statement and recommendations of the International Ankle Consortium. *Br J Sports Med.* 2018;52(20):1304–1310. doi:10.1136/bjsports-2017-098885
34. Mollon B, Wasserstein D, Murphy GM, White LM, Theodoropoulos J. High ankle sprains in professional ice hockey players: prognosis and correlation between magnetic resonance imaging patterns of injury and return to play. *Orthop J Sports Med.* 2019;7(9):2325967119871578. doi:10.1177/2325967119871578
35. Holmes RD, Yan YY, Mallinson PI, Andrews GT, Munk PL, Ouellette HA. Imaging review of hockey-related lower extremity injuries. *Semin Musculoskelet Radiol.* 2022;26(1):13–27. doi:10.1055/s-0041-1731795
36. van Rijn RM, van Os AG, Bernsen RM, Luijsterburg PA, Koes BW, Bierma-Zeinstra SM. What is the clinical course of acute ankle sprains? A systematic literature review. *Am J Med.* 2008;121(4):324–331 e326. doi:10.1016/j.amjmed.2007.11.018
37. Lai MWW, Sit RWS. Healing of complete tear of the anterior talofibular ligament and early ankle stabilization after autologous platelet rich plasma: a case report and literature review. *Arch Bone Jt Surg.* 2018;6(2):146–149.
38. Michels F, Pereira H, Calder J, et al. Searching for consensus in the approach to patients with chronic lateral ankle instability: ask the expert. *Knee Surg Sports Traumatol Arthrosc.* 2018;26(7):2095–2102. doi:10.1007/s00167-017-4556-0
39. Bosien WR, Staples OS, Russell SW. Residual disability following acute ankle sprains. *J Bone Joint Surg Am.* 1955;37-A(6):1237–1243. doi:10.2106/00004623-195537060-00011
40. Hadeed MM, Dempsey IJ, Tyrrell Burrus M, et al. Predictors of osteochondral lesions of the talus in patients undergoing Brostrom-Gould ankle ligament reconstruction. *J Foot Ankle Surg.* 2020;59(1):21–26. doi:10.1053/j.jfas.2018.05.006
41. Takao M, Uchio Y, Naito K, Fukazawa I, Ochi M. Arthroscopic assessment for intra-articular disorders in residual ankle disability after sprain. *Am J Sports Med.* 2005;33(5):686–692. doi:10.1177/0363546504270566
42. Bezuglov E, Khaitin V, Lazarev A, et al. Asymptomatic foot and ankle abnormalities in elite professional soccer players. *Orthop J Sports Med.* 2021;9(1):2325967120979994. doi:10.1177/2325967120979994
43. Weber MA, Wunnemann F, Jungmann PM, Kuni B, Rehnitz C. Modern cartilage imaging of the ankle. *Rofo.* 2017;189(10):945–956. doi:10.1055/s-0043-110861
44. Elias I, Zoga AC, Morrison WB, Besser MP, Schweitzer ME, Raikin SM. Osteochondral lesions of the talus: localization and morphologic data from 424 patients using a novel anatomical grid scheme. *Foot Ankle Int.* 2007;28(2):154–161. doi:10.3113/FAI.2007.0154
45. Zengerink M, Struijs PA, Tol JL, van Dijk CN. Treatment of osteochondral lesions of the talus: a systematic review. *Knee Surg Sports Traumatol Arthrosc.* 2010;18(2):238–246. doi:10.1007/s00167-009-0942-6
46. DeJong AF, Fish PN, Hertel J. Running behaviors, motivations, and injury risk during the COVID-19 pandemic: a survey of 1147 runners. *PLoS One.* 2021;16(2):e0246300. doi:10.1371/journal.pone.0246300
47. van Aert GJJ, van der Laan L, Boonman-de Winter LJM, et al. Effect of the COVID-19 pandemic during the first lockdown in the Netherlands on the number of trauma-related admissions, trauma severity and treatment: the results of a retrospective cohort study in a level 2 trauma centre. *BMJ Open.* 2021;11(2):e045015. doi:10.1136/bmjopen-2020-045015
48. Lim MA, Mulyadi Ridia KG, Pranata R. Epidemiological pattern of orthopaedic fracture during the COVID-19 pandemic: a systematic review and meta-analysis. *J Clin Orthop Trauma.* 2021;16:16–23. doi:10.1016/j.jcot.2020.12.028
49. Nia A, Popp D, Diendorfer C, et al. Impact of lockdown during the COVID-19 pandemic on number of patients and patterns of injuries at a level I trauma center. *Wien Klin Wochenschr.* 2021;133:336–343. doi:10.1007/s00508-021-01824-z
50. Bazett-Jones DM, Garcia MC, Taylor-Haas JA, et al. Impact of COVID-19 social distancing restrictions on training habits, injury, and care seeking behavior in youth long-distance runners. *Front Sports Act Living.* 2020;2:586141. doi:10.3389/fspor.2020.586141
51. Sephton BM, Mahapatra P, Shenouda M, et al. The effect of COVID-19 on a Major Trauma Network. An analysis of mechanism of injury pattern, referral load and operative case-mix. *Injury.* 2021;52(3):395–401. doi:10.1016/j.injury.2021.02.035
52. Wenning M, Gehring D, Lange T, et al. Clinical evaluation of manual stress testing, stress ultrasound and 3D stress MRI in chronic mechanical ankle instability. *BMC Musculoskelet Disord.* 2021;22(1):198. doi:10.1186/s12891-021-03998-z
53. Beckenkamp PR, Lin CC, Macaskill P, Michaleff ZA, Maher CG, Moseley AM. Diagnostic accuracy of the Ottawa Ankle and Midfoot Rules: a systematic review with meta-analysis. *Br J Sports Med.* 2017;51(6):504–510. doi:10.1136/bjsports-2016-096858
54. Lehtola R, Leskela HV, Flinkkila T, et al. Suture button versus syndesmosis screw fixation in pronation-external rotation ankle fractures: a minimum 6-year follow-up of a randomised controlled trial. *Injury.* 2021;52:3143–3149. doi:10.1016/j.injury.2021.06.025
55. Brandenburg LS, Siegel M, Neubauer J, Merz J, Bode G, Kuhle J. Measuring standing hindfoot alignment: reliability of different approaches in conventional x-ray and cone-beam CT. *Arch Orthop Trauma Surg.* 2021;142:3035–3043. doi:10.1007/s00402-021-03904-1
56. Naqvi GA, Cunningham P, Lynch B, Galvin R, Awan N. Fixation of ankle syndesmotic injuries: comparison of tightrope fixation and syndesmotic screw fixation for accuracy of syndesmotic reduction. *Am J Sports Med.* 2012;40(12):2828–2835. doi:10.1177/0363546512461480
57. Forschner PF, Beitzel K, Imhoff AB, et al. Five-year outcomes after treatment for acute instability of the tibiofibular syndesmosis using a suture-button fixation system. *Orthop J Sports Med.* 2017;5(4):2325967117702854. doi:10.1177/2325967117702854
58. Rodrigues JC, Santos ALG, Prado MP, et al. Comparative CT with stress manoeuvres for diagnosing distal isolated tibiofibular syndesmotic injury in acute ankle sprain: a protocol for an accuracy- test prospective study. *BMJ Open.* 2020;10(9):e037239. doi:10.1136/bmjopen-2020-037239
59. Vetter SY, Euler J, Beisemann N, et al. Validation of radiological reduction criteria with intraoperative cone beam CT in unstable syndesmotic injuries. *Eur J Trauma Emerg Surg.* 2021;47(4):897–903. doi:10.1007/s00068-020-01299-z
60. Rammelt S, Zwipp H, Grass R. Injuries to the distal tibiofibular syndesmosis: an evidence-based approach to acute and chronic lesions. *Foot Ankle Clin.* 2008;13(4):611–633, vii–viii. doi:10.1016/j.fcl.2008.08.001
61. Patel S, Malhotra K, Cullen NP, Singh D, Goldberg AJ, Welck MJ. Defining reference values for the normal tibiofibular syndesmosis in adults using weight-bearing CT. *Bone Joint J.* 2019;101-B(3):348–352. doi:10.1302/0301-620X.101B3.BJJ-2018-0829.R1
62. Hickie J, Walstra F, Duggan P, Ouellette H, Munk P, Mallinson P. Dual-energy CT characterization of winter sports injuries. *Br J Radiol.* 2020;93(1106):20190620. doi:10.1259/bjr.20190620

63. Do TD, Sawall S, Heinze S, et al. A semi-automated quantitative comparison of metal artifact reduction in photon-counting computed tomography by energy-selective thresholding. *Sci Rep*. 2020;10(1):21099. doi:10.1038/s41598-020-77904-3
64. Hsieh SS, Leng S, Rajendran K, Tao S, McCollough CH. Photon counting CT: clinical applications and future developments. *IEEE Trans Radiat Plasma Med Sci*. 2021;5(4):441–452. doi:10.1109/TRPMS.2020.3020212
65. Foti G, Guerriero M, Faccioli N, et al. Identification of bone marrow edema around the ankle joint in non-traumatic patients: diagnostic accuracy of dual-energy computed tomography. *Clin Imaging*. 2021;69:341–348. doi:10.1016/j.clinimag.2020.09.013
66. Foti G, Catania M, Caia S, et al. Identification of bone marrow edema of the ankle: diagnostic accuracy of dual-energy CT in comparison with MRI. *Radiol Med*. 2019;124(10):1028–1036. doi:10.1007/s11547-019-01062-4
67. Allahabadi S, Amendola A, Lau BC. Optimizing return to play for common and controversial foot and ankle sports injuries. *JBJS Rev*. 2020;8(12):e20.00067. doi:10.2106/JBJS.RVW.20.00067
68. Gersing AS, Schwaiger BJ, Wortler K, Jungmann PM. Dezidierte Knorpelbildgebung zur Detektion von Knorpelverletzungen und osteochondralen Läsionen [Advanced cartilage imaging for detection of cartilage injuries and osteochondral lesions]. *Radiologe*. 2018;58(5):422–432. German. doi:10.1007/s00117-017-0348-2
69. Hermans JJ, Beumer A, Hop WC, Moonen AF, Ginai AZ. Tibiofibular syndesmosis in acute ankle fractures: additional value of an oblique MR image plane. *Skeletal Radiol*. 2012;41(2):193–202. doi:10.1007/s00256-011-1179-2
70. Duc SR, Mengiardi B, Pfirrmann CW, Hodler J, Zanetti M. Improved visualization of collateral ligaments of the ankle: multiplanar reconstructions based on standard 2D turbo spin-echo MR images. *Eur Radiol*. 2007;17(5):1162–1171. doi:10.1007/s00330-006-0427-7
71. Kim M, Choi YS, Jeong MS, et al. Comprehensive assessment of ankle syndesmosis injury using 3D isotropic turbo spin-echo sequences: diagnostic performance compared with that of conventional and oblique 3-T MRI. *AJR Am J Roentgenol*. 2017;208(4):827–833. doi:10.2214/AJR.16.16985
72. Randell M, Marsland D, Ballard E, Forster B, Lutz M. MRI for high ankle sprains with an unstable syndesmosis: posterior malleolus bone oedema is common and time to scan matters. *Knee Surg Sports Traumatol Arthrosc*. 2019;27(9):2890–2897. doi:10.1007/s00167-019-05581-5
73. Theysohn JM, Kraff O, Maderwald S, et al. MRI of the ankle joint in healthy non-athletes and in marathon runners: image quality issues at 7.0 T compared to 1.5 T. *Skeletal Radiol*. 2013;42(2):261–267. doi:10.1007/s00256-012-1454-x
74. Kirschke JS, Braun S, Baum T, et al. Diagnostic value of CT arthrography for evaluation of osteochondral lesions at the ankle. *Biomed Res Int*. 2016;2016:3594253. doi:10.1155/2016/3594253
75. Jungmann PM, Agten CA, Pfirrmann CW, Sutter R. Advances in MRI around metal. *J Magn Reson Imaging*. 2017;46(4):972–991. doi:10.1002/jmri.25708
76. de Cesar Netto C, Fonseca LF, Fritz B, et al. Metal artifact reduction MRI of total ankle arthroplasty implants. *Eur Radiol*. 2018;28(5):2216–2227. doi:10.1007/s00330-017-5153-9
77. Jungmann PM, Ganter C, Schaeffeler CJ, et al. View-angle tilting and slice-encoding metal artifact correction for artifact reduction in MRI: experimental sequence optimization for orthopaedic tumor endoprostheses and clinical application. *PLoS One*. 2015;10(4):e0124922. doi:10.1371/journal.pone.0124922
78. Jungmann PM, Bensler S, Zingg P, Fritz B, Pfirrmann CW, Sutter R. Improved visualization of juxta prosthetic tissue using metal artifact reduction magnetic resonance imaging: experimental and clinical optimization of compressed sensing SEMAC. *Invest Radiol*. 2019;54(1):23–31. doi:10.1097/RLI.0000000000000504
79. Baur OL, Den Harder JM, Hemke R, et al. The road to optimal acceleration of Dixon imaging and quantitative T2-mapping in the ankle using compressed sensing and parallel imaging. *Eur J Radiol*. 2020;132:109295. doi:10.1016/j.ejrad.2020.109295
80. Gersing AS, Bodden J, Neumann J, et al. Accelerating anatomical 2D turbo spin echo imaging of the ankle using compressed sensing. *Eur J Radiol*. 2019;118:277–284. doi:10.1016/j.ejrad.2019.06.006
81. Hur ES, Bohl DD, Lee S. Lateral ligament instability: review of pathology and diagnosis. *Curr Rev Musculoskelet Med*. 2020;13(4):494–500. doi:10.1007/s12178-020-09641-z
82. Tan DW, Teh DJW, Chee YH. Accuracy of magnetic resonance imaging in diagnosing lateral ankle ligament injuries: a comparative study with surgical findings and timings of scans. *Asia Pac J Sports Med Arthrosc Rehabil Technol*. 2017;7:15–20. doi:10.1016/j.asmart.2016.09.003
83. Liu W, Li H, Hua Y. Quantitative magnetic resonance imaging (MRI) analysis of anterior talofibular ligament in lateral chronic ankle instability ankles pre- and postoperatively. *BMC Musculoskelet Disord*. 2017;18(1):397. doi:10.1186/s12891-017-1758-z
84. Li HY, Li WL, Chen SY, Hua YH. Increased ATFL-PTFL angle could be an indirect MRI sign in diagnosis of chronic ATFL injury. *Knee Surg Sports Traumatol Arthrosc*. 2020;28(1):208–212. doi:10.1007/s00167-018-5252-4
85. Ahn J, Choi JG, Jeong BO. The signal intensity of preoperative magnetic resonance imaging has predictive value for determining the arthroscopic reparability of the anterior talofibular ligament. *Knee Surg Sports Traumatol Arthrosc*. 2021;29(5):1535–1543. doi:10.1007/s00167-020-06208-w
86. Li H, Hua Y, Feng S, Li H, Chen S. Lower signal intensity of the anterior talofibular ligament is associated with a higher rate of return to sport after ATFL repair for chronic lateral ankle instability. *Am J Sports Med*. 2019;47(10):2380–2385. doi:10.1177/0363546519858588
87. Li Q, Ma K, Tao H, et al. Clinical and magnetic resonance imaging assessment of anatomical lateral ankle ligament reconstruction: comparison of tendon allograft and autograft. *Int Orthop*. 2018;42(3):551–557. doi:10.1007/s00264-018-3802-5
88. Crema MD, Krivokapic B, Guermazi A, et al. MRI of ankle sprain: the association between joint effusion and structural injury severity in a large cohort of athletes. *Eur Radiol*. 2019;29(11):6336–6344. doi:10.1007/s00330-019-06156-1
89. Elias I, Raikin SM, Schweitzer ME, Besser MP, Morrison WB, Zoga AC. Osteochondral lesions of the distal tibial plafond: localization and morphologic characteristics with an anatomical grid. *Foot Ankle Int*. 2009;30(6):524–529. doi:10.3113/FAI.2009.0524
90. Boutin RD, Chang J, Bateni C, Giza E, Wisner ER, Yao L. The notch of Harty (pseudodeflect of the tibial plafond): frequency and characteristic findings at MRI of the ankle. *AJR Am J Roentgenol*. 2015;205(2):358–363. doi:10.2214/AJR.14.14012
91. Schmid MR, Pfirrmann CW, Hodler J, Vienne P, Zanetti M. Cartilage lesions in the ankle joint: comparison of MR arthrography and CT arthrography. *Skeletal Radiol*. 2003;32(5):259–265. doi:10.1007/s00256-003-0628-y
92. Yasui Y, Hannon CP, Fraser EJ, et al. Lesion size measured on MRI does not accurately reflect arthroscopic measurement in talar osteochondral lesions. *Orthop J Sports Med*. 2019;7(2):2325967118825261. doi:10.1177/2325967118825261

93. Berndt AL, Harty M. Transchondral fractures (osteochondritis dissecans) of the talus. *J Bone Joint Surg Am*. 1959;41-A:988–1020. doi:10.2106/00004623-195941060-00002
94. Dipaola JD, Nelson DW, Colville MR. Characterizing osteochondral lesions by magnetic resonance imaging. *Arthroscopy*. 1991;7(1):101–104. doi:10.1016/0749-8063(91)90087-E
95. Nelson DW, DiPaola J, Colville M, Schmidgall J. Osteochondritis dissecans of the talus and knee: prospective comparison of MR and arthroscopic classifications. *J Comput Assist Tomogr*. 1990;14(5):804–808. doi:10.1097/00004728-199009000-00026
96. Korner D, Kohler P, Schroter S, et al. Pain in osteochondral lesions of the ankle - an investigation based on data from the German Cartilage Registry (KnorpelRegister DGOU). *Z Orthop Unfall*. 2018;156(2):160–167. doi:10.1055/s-0043-124597
97. Griffith JF, Lau DT, Yeung DK, Wong MW. High-resolution MR imaging of talar osteochondral lesions with new classification. *Skeletal Radiol*. 2012;41(4):387–399. doi:10.1007/s00256-011-1246-8
98. Szaro P, Geijer M, Solidakis N. Traumatic and non-traumatic bone marrow edema in ankle MRI: a pictorial essay. *Insights Imaging*. 2020;11(1):97. doi:10.1186/s13244-020-00900-8
99. van Ochten JM, de Vries AD, van Putte N, et al. Association between patient history and physical examination and osteoarthritis after ankle sprain. *Int J Sports Med*. 2017;38(9):717–724. doi:10.1055/s-0043-109554
100. Passon T, Germann C, Fritz B, Pfirrmann C, Sutter R. Bone marrow edema of the medioplantar talar head is associated with severe ligamentous injury in ankle sprain. *Skeletal Radiol*. 2022;51(10):1937–1946. doi:10.1007/s00256-022-04043-3
101. Peterfy CG, Guermazi A, Zaim S, et al. Whole-Organ Magnetic Resonance Imaging Score (WORMS) of the knee in osteoarthritis. *Osteoarthritis Cartilage*. 2004;12(3):177–190. doi:10.1016/j.joca.2003.11.003
102. Jungmann PM, Gersing AS, Woertler K, et al. Reliable semiquantitative whole-joint MRI score for the shoulder joint: the shoulder osteoarthritis severity (SOAS) score. *J Magn Reson Imaging*. 2019;49(7):e152–e163. doi:10.1002/jmri.26251
103. Neumann J, Zhang AL, Schwaiger BJ, et al. Validation of scoring Hip osteoarthritis with MRI (SHOMRI) scores using Hip arthroscopy as a standard of reference. *Eur Radiol*. 2019;29(2):578–587. doi:10.1007/s00330-018-5623-8
104. Schmal H, Pilz IH, Henkelmann R, Salzmann GM, Sudkamp NP, Niemeyer P. Association between intraarticular cytokine levels and clinical parameters of osteochondritis dissecans in the ankle. *BMC Musculoskelet Disord*. 2014;15:169. doi:10.1186/1471-2474-15-169
105. Dunn A. The pre-signing medical examination: the radiologists' role. *Eur J Radiol*. 2019;118:239–244. doi:10.1016/j.ejrad.2019.07.017
106. Behzadi C, Maas KJ, Welsch G, et al. Quantitative T2 \* relaxation time analysis of articular cartilage of the tibiotalar joint in professional football players and healthy volunteers at 3T MRI. *J Magn Reson Imaging*. 2018;47(2):372–379. doi:10.1002/jmri.25757
107. Kim HK, Mirjalili A, Doyle A, Fernandez J. Tibiotalar cartilage stress corresponds to T2 mapping: application to barefoot running in novice and marathon-experienced runners. *Comput Methods Biomech Biomed Engin*. 2019;22(14):1153–1161. doi:10.1080/10255842.2019.1645133
108. Hu Y, Tao H, Qiao Y, et al. Evaluation of the talar cartilage in chronic lateral ankle instability with lateral ligament injury using biochemical T2\* mapping: correlation with clinical symptoms. *Acad Radiol*. 2018;25(11):1415–1421. doi:10.1016/j.acra.2018.01.021
109. Kim HS, Yoon YC, Sung KS, Kim MJ, Ahn S. Comparison of T2 relaxation values in subtalar cartilage between patients with lateral instability of the ankle joint and healthy volunteers. *Eur Radiol*. 2018;28(10):4151–4162. doi:10.1007/s00330-018-5390-6
110. Park SY, Yoon YC, Cha JG, Sung KS. T2 relaxation values of the talar trochlear articular cartilage: comparison between patients with lateral instability of the ankle joint and healthy volunteers. *AJR Am J Roentgenol*. 2016;206(1):136–143. doi:10.2214/AJR.15.14364
111. Tao H, Hu Y, Qiao Y, et al. T2 -Mapping evaluation of early cartilage alteration of talus for chronic lateral ankle instability with isolated anterior talofibular ligament tear or combined with calcaneofibular ligament tear. *J Magn Reson Imaging*. 2018;47(1):69–77. doi:10.1002/jmri.25745
112. Tao H, Hu Y, Lu R, et al. Impact of chronic lateral ankle instability with lateral collateral ligament injuries on biochemical alterations in the cartilage of the subtalar and midtarsal joints based on MRI T2 mapping. *Korean J Radiol*. 2021;22(3):384–394. doi:10.3348/kjr.2020.0021
113. Rehnitz C, Kuni B, Wuenemann F, et al. Delayed gadolinium-enhanced MRI of cartilage (dGEMRIC) and T2 mapping of talar osteochondral lesions: indicators of clinical outcomes. *J Magn Reson Imaging*. 2017;46(6):1601–1610. doi:10.1002/jmri.25731
114. Hu Y, Zhang Y, Li Q, et al. Magnetic resonance imaging T2\* mapping of the talar dome and subtalar joint cartilage 3 years after anterior talofibular ligament repair or reconstruction in chronic lateral ankle instability. *Am J Sports Med*. 2021;49(3):737–746. doi:10.1177/0363546520982240
115. Jerban S, Chang DG, Ma Y, Jang H, Chang EY, Du J. An update in qualitative imaging of bone using ultrashort echo time magnetic resonance. *Front Endocrinol (Lausanne)*. 2020;11:555756. doi:10.3389/fendo.2020.555756
116. Gersing AS, Pfeiffer D, Kopp FK, et al. Evaluation of MR-derived CT-like images and simulated radiographs compared to conventional radiography in patients with benign and malignant bone tumors. *Eur Radiol*. 2019;29(1):13–21. doi:10.1007/s00330-018-5450-y
117. Nordeck SM, Koerper CE, Adler A, et al. Simulated radiographic bone and joint modeling from 3D ankle MRI: feasibility and comparison with radiographs and 2D MRI. *Skeletal Radiol*. 2017;46(5):651–664. doi:10.1007/s00256-017-2596-7
118. Chang EY, Du J, Chung CB. UTE imaging in the musculoskeletal system. *J Magn Reson Imaging*. 2015;41(4):870–883. doi:10.1002/jmri.24713
119. Schwaiger BJ, Schneider C, Kronthaler S, et al. CT-like images based on T1 spoiled gradient-echo and ultra-short echo time MRI sequences for the assessment of vertebral fractures and degenerative bone changes of the spine. *Eur Radiol*. 2021;31(7):4680–4689. doi:10.1007/s00330-020-07597-9
120. Lu X, Jerban S, Wan L, et al. Three-dimensional ultrashort echo time imaging with tricomponent analysis for human cortical bone. *Magn Reson Med*. 2019;82(1):348–355. doi:10.1002/mrm.27718
121. Siriwanarangsun P, Bae WC, Statum S, Chung CB. Advanced MRI techniques for the ankle. *AJR Am J Roentgenol*. 2017;209(3):511–524. doi:10.2214/AJR.17.18057
122. Wiesinger F, Sacolick LI, Menini A, et al. Zero TE MR bone imaging in the head. *Magn Reson Med*. 2016;75(1):107–114. doi:10.1002/mrm.25545
123. Breighner RE, Bogner EA, Lee SC, Koff MF, Potter HG. Evaluation of osseous morphology of the hip using zero echo time magnetic resonance imaging. *Am J Sports Med*. 2019;47(14):3460–3468. doi:10.1177/0363546519878170
124. Breighner RE, Endo Y, Konin GP, Gulotta LV, Koff MF, Potter HG. technical developments: zero echo time imaging of the shoulder: enhanced osseous detail by using MR imaging. *Radiology*. 2018;286(3):960–966. doi:10.1148/radiol.2017170906



125. Larson PE, Han M, Krug R, et al. Ultrashort echo time and zero echo time MRI at 7T. *MAGMA*. 2016;29(3):359–370. doi:10.1007/s10334-015-0509-0
126. Sandberg JK, Young VA, Yuan J, Hargreaves BA, Wishah F, Vasanawala SS. Zero echo time pediatric musculoskeletal magnetic resonance imaging: initial experience. *Pediatr Radiol*. 2021;51:2549–2560. doi:10.1007/s00247-021-05125-5
127. de Mello RAF, Ma YJ, Ashir A, et al. Three-dimensional zero echo time magnetic resonance imaging versus 3-dimensional computed tomography for glenoid bone assessment. *Arthroscopy*. 2020;36(9):2391–2400. doi:10.1016/j.arthro.2020.05.042
128. Baltes TPA, Arnaiz J, Geertsema L, et al. Diagnostic value of ultrasonography in acute lateral and syndesmotic ligamentous ankle injuries. *Eur Radiol*. 2021;31(4):2610–2620. doi:10.1007/s00330-020-07305-7
129. Fritz B, Fritz J. MR imaging-ultrasonography correlation of acute and chronic foot and ankle conditions. *Magn Reson Imaging Clin N Am*. 2023;31(2):321–335. doi:10.1016/j.mric.2023.01.009
130. Ergun T, Peker A, Aybay MN, Turan K, Muratoglu OG, Cabuk H. Ultrasonography view for acute ankle injury: comparison of ultrasonography and magnetic resonance imaging. *Arch Orthop Trauma Surg*. 2023;143(3):1531–1536. doi:10.1007/s00402-022-04553-8
131. Kaminski TW, Hertel J, Amendola N, et al. National Athletic Trainers' Association position statement: conservative management and prevention of ankle sprains in athletes. *J Athl Train*. 2013;48(4):528–545. doi:10.4085/1062-6050-48.4.02
132. Biz C, Nicoletti P, Tomasin M, Bragazzi NL, Di Rubbo G, Ruggieri P. Is kinesio taping effective for sport performance and ankle function of athletes with Chronic Ankle Instability (CAI)? A systematic review and meta-analysis. *Medicina*. 2022;58(5):210.
133. Stenquist DS, Ye MY, Kwon JY. Acute and chronic syndesmotic instability: role of surgical stabilization. *Clin Sports Med*. 2020;39(4):745–771. doi:10.1016/j.csm.2020.06.002
134. Kim SW, Jung HG, Lee JS. Ligament stabilization improved clinical and radiographic outcomes for individuals with chronic ankle instability and medial ankle osteoarthritis. *Knee Surg Sports Traumatol Arthrosc*. 2020;28(10):3294–3300. doi:10.1007/s00167-020-05845-5
135. Park S, Kim T, Lee M, Park Y. Absence of ATFL remnant does not affect the clinical outcomes of the modified brostrom operation for chronic ankle instability. *Knee Surg Sports Traumatol Arthrosc*. 2020;28(1):213–220. doi:10.1007/s00167-019-05464-9
136. Li H, Hua Y, Li H, Ma K, Li S, Chen S. Activity level and function 2 years after anterior talofibular ligament repair: a comparison between arthroscopic repair and open repair procedures. *Am J Sports Med*. 2017;45(9):2044–2051. doi:10.1177/0363546517698675
137. Li H, Zhao Y, Hua Y, Li Q, Li H, Chen S. Knotless anchor repair produced similarly favourable outcomes as knot anchor repair for anterior talofibular ligament repair. *Knee Surg Sports Traumatol Arthrosc*. 2020;28(12):3987–3993. doi:10.1007/s00167-020-05998-3
138. Li H, Hua Y, Li H, Chen S. Anterior talofibular ligament (ATFL) repair using two suture anchors produced better functional outcomes than using one suture anchor for the treatment of chronic lateral ankle instability. *Knee Surg Sports Traumatol Arthrosc*. 2020;28(1):221–226. doi:10.1007/s00167-019-05550-y
139. Li H, Hua Y, Li H, Chen S. Anatomical reconstruction produced similarly favorable outcomes as repair procedures for the treatment of chronic lateral ankle instability at long-term follow-up. *Knee Surg Sports Traumatol Arthrosc*. 2020;28(10):3324–3329. doi:10.1007/s00167-018-5176-z
140. Seo SG, Kim JS, Seo DK, Kim YK, Lee SH, Lee HS. Osteochondral lesions of the talus. *Acta Orthop*. 2018;89(4):462–467. doi:10.1080/17453674.2018.1460777
141. Vannini F, Costa GG, Caravelli S, Pagliuzzi G, Mosca M. Treatment of osteochondral lesions of the talus in athletes: what is the evidence? *Joints*. 2016;4(2):111–120. doi:10.11138/jts/2016.4.2.111
142. Rikken QGH, Kerkhoffs G. Osteochondral lesions of the talus: an individualized treatment paradigm from the Amsterdam perspective. *Foot Ankle Clin*. 2021;26(1):121–136. doi:10.1016/j.fcl.2020.10.002
143. O'Loughlin PF, Heyworth BE, Kennedy JG. Current concepts in the diagnosis and treatment of osteochondral lesions of the ankle. *Am J Sports Med*. 2010;38(2):392–404. doi:10.1177/0363546509336336
144. Shimozono Y, Hurley ET, Myerson CL, Kennedy JG. Good clinical and functional outcomes at mid-term following autologous osteochondral transplantation for osteochondral lesions of the talus. *Knee Surg Sports Traumatol Arthrosc*. 2018;26(10):3055–3062. doi:10.1007/s00167-018-4917-3
145. Choi GW, Choi WJ, Youn HK, Park YJ, Lee JW. Osteochondral lesions of the talus: are there any differences between osteochondral and chondral types? *Am J Sports Med*. 2013;41(3):504–510. doi:10.1177/0363546512472976
146. Roth KE, Ossendorff R, Klos K, Simons P, Drees P, Salzmänn GM. Arthroscopic minced cartilage implantation for chondral lesions at the talus: a technical note. *Arthrosc Tech*. 2021;10(4):e1149–e1154. doi:10.1016/j.eats.2021.01.006
147. Ruther H, Seif Amir Hosseini A, Frosch S, et al. Refixation von osteochondralen Fragmenten mit resorbierbaren Polylactid-Implantaten [Refixation of osteochondral fragments with resorbable polylactid implants: long-term clinical and MRI results]. *Unfallchirurg*. 2020;123(10):797–806. German. doi:10.1007/s00113-020-00798-3
148. Gottschalk O, Altenberger S, Baumbach S, et al. Functional medium-term results after autologous matrix-induced chondrogenesis for osteochondral lesions of the talus: a 5-year prospective cohort study. *J Foot Ankle Surg*. 2017;56(5):930–936. doi:10.1053/j.jfas.2017.05.002
149. Shimozono Y, Donders JCE, Yasui Y, et al. Effect of the containment type on clinical outcomes in osteochondral lesions of the talus treated with autologous osteochondral transplantation. *Am J Sports Med*. 2018;46(9):2096–2102. doi:10.1177/0363546518776659
150. Becher C, Malahias MA, Ali MM, Maffulli N, Thermann H. Arthroscopic microfracture vs. arthroscopic autologous matrix-induced chondrogenesis for the treatment of articular cartilage defects of the talus. *Knee Surg Sports Traumatol Arthrosc*. 2019;27(9):2731–2736. doi:10.1007/s00167-018-5278-7
151. Yang HY, Lee KB. Arthroscopic microfracture for osteochondral lesions of the talus: second-look arthroscopic and magnetic resonance analysis of cartilage repair tissue outcomes. *J Bone Joint Surg Am*. 2020;102(1):10–20. doi:10.2106/JBJS.19.00208
152. Weigelt L, Hartmann R, Pfirrmann C, Espinosa N, Wirth SH. Autologous matrix-induced chondrogenesis for osteochondral lesions of the talus: a clinical and radiological 2- to 8-year follow-up study. *Am J Sports Med*. 2019;47(7):1679–1686. doi:10.1177/0363546519841574
153. Uselli FG, D'Ambrosi R, Maccario C, Boga M, de Girolamo L. All-arthroscopic AMIC((R)) (AT-AMIC((R))) technique with autologous bone graft for talar osteochondral defects: clinical and radiological results. *Knee Surg Sports Traumatol Arthrosc*. 2018;26(3):875–881. doi:10.1007/s00167-016-4318-4
154. Toale J, Shimozono Y, Mulvin C, Dahmen J, Kerkhoffs G, Kennedy JG. Midterm outcomes of bone marrow stimulation for primary osteochondral lesions of the talus: a systematic review. *Orthop J Sports Med*. 2019;7(10):2325967119879127. doi:10.1177/2325967119879127

155. Shimozone Y, Hurley ET, Yasui Y, Deyer TW, Kennedy JG. The presence and degree of bone marrow edema influence midterm clinical outcomes after microfracture for osteochondral lesions of the talus. *Am J Sports Med.* 2018;46(10):2503–2508. doi:10.1177/0363546518782701
156. Shimozone Y, Coale M, Yasui Y, O'Halloran A, Deyer TW, Kennedy JG. Subchondral bone degradation after microfracture for osteochondral lesions of the talus: an MRI analysis. *Am J Sports Med.* 2018;46(3):642–648. doi:10.1177/0363546517739606
157. Chan KW, Ferkel RD, Kern B, Chan SS, Applegate GR. Correlation of MRI appearance of autologous chondrocyte implantation in the ankle with clinical outcome. *Cartilage.* 2018;9(1):21–29. doi:10.1177/1947603516681131
158. Nguyen A, Ramasamy A, Walsh M, McMenemy L, Calder JDF. Autologous osteochondral transplantation for large osteochondral lesions of the talus is a viable option in an athletic population. *Am J Sports Med.* 2019;47(14):3429–3435. doi:10.1177/0363546519881420

Open Access Journal of Sports Medicine

Dovepress

### Publish your work in this journal

Open Access Journal of Sports Medicine is an international, peer-reviewed, open access journal publishing original research, reports, reviews and commentaries on all areas of sports medicine. The manuscript management system is completely online and includes a very quick and fair peer-review system. Visit <http://www.dovepress.com/testimonials.php> to read real quotes from published authors.

Submit your manuscript here: <http://www.dovepress.com/open-access-journal-of-sports-medicine-journal>